Electric Power Systems Research 96 (2013) 157–169

Contents lists available at SciVerse ScienceDirect

Electric Power Systems Research

journal homepage: www.elsevier.com/locate/epsr

Indirect matrix converter with unity voltage transfer ratio for AC to AC power conversion

Alireza Jahangiri *, Ahmad Radan

Electrical Engineering Faculty, K.N. Toosi University of Technology, Seyedkhandan Bridge, 1431714191 Tehran, Iran

ARTICLE INFO

Article history:
Received 26 July 2012
Received in revised form
13 November 2012
Accepted 14 November 2012
Available online 17 December 2012

Keywords:
Indirect matrix converter
Unity voltage transfer ratio
AC/AC boost chopper

ABSTRACT

Having a voltage transfer ratio lower than unity with a 0.866 upper limit, even lower than 0.866 in the course of experiments because of parasitic components of real power circuits, is one of the shortcomings of matrix converters. This deficiency is one of the greatest impediments to industry adaptation of matrix converters. To surmount this barrier this paper proposes a novel modification in circuit topology of indirect matrix converters (IMC) achieving voltage boosting and unity voltage transfer ratio. Besides preserving the inherent advantages of the conventional matrix converters, such as controllability of input power factor, sinusoidal input/output currents and the ability of bidirectional power flow, the remarkable feature of this solution is that, unlike the other research in this field no special control strategy or additional reactive elements at the DC-link is used and the integrity of the converter has been kept as much as possible. Furthermore a new efficient switching strategy is proposed for the new converter. Simulation results are shown to support the given theoretical analyses and experimental results obtained from a 5 kW converter verify the full functionality of the proposed topology.

1. Introduction

The development trend of power electronic converters for AC to AC power conversions is to integrate the frequency converter and other parts of equipment into a single unit to reduce volume and costs and to increase the overall efficiency and reliability. Apart from the AC to DC to AC conversion system used in many conventional converter applications with huge reactive elements at the intermediate DC bus, the well-known direct matrix converter (DMC) first introduced in 1979 [1] and shown in Fig. 1(a), can directly convert AC to AC without any necessity to a large reactive element. DMCs hold many advantages, including an adjustable input power factor, bidirectional power flow, high-quality power output waveforms, and the potential of a more compact product because they do not require a large energy storage compartment, such as a DC bus capacitor and through this the converter can be integrated to electrical motors. Despite these benefits, however, the DMC has not been adopted by industry. This is mainly because of the modulation algorithm of these converters requires a complex and difficult pulse width modulation (PWM) switching strategy being prone to commutation failure. An alternative topology for AC/AC conversion, known as IMC topology, is shown in Fig. 1(b). The IMC consists of two separated line and load bridges and offers the same benefits as the DMC, but it also provides an option to reduce the number of active switches of the line bridge to three if no bidirectional power flow is needed and eliminates the commutation problems related to DMCs [2–5]. Several papers have been published to illustrate this topology. In [2], this topology is treated as a rectifier/inverter, in which line and load side switches are controlled separately. Some papers [3–8] treat this topology as a type of matrix converter. In them, a detailed PWM control method is proposed with synchronized switching of the both line and load side switches.

However, the main shortcoming of matrix converters is limitation of voltage transfer ratio to 0.866, being theoretically the highest achievable ratio between the output and input voltages. A low voltage transfer ratio not only limits the applications of this converter in power systems, but also causes the output current to become higher for a certain output power leading to an increase of both load and converter losses, as a consequence. There are some discussions to improve the voltage transfer ratio in matrix converters. One of the simplest solutions is to improve the voltage transfer ratio by feeding the converter from the power supply through a transformer. However, as the commercial transformers applied in the power grid frequency are costly and bulky, this solution does not seem reasonable. In [9], the proposal is to use the matrix converter in overmodulation region in order to improve the voltage gain. The voltage transfer ratio successfully improved to 0.95 through this solution. But, the output currents contain large

* Corresponding author. Tel.: +98 21 88462408; fax: +98 21 88462066.
E-mail addresses: jahangiri@ee.kntu.ac.ir, jahangiri87@yahoo.com (A. Jahangiri), radan@kntu.ac.ir (A. Radan).

0378-7796/$ – see front matter
http://dx.doi.org/10.1016/j.epsr.2012.11.008

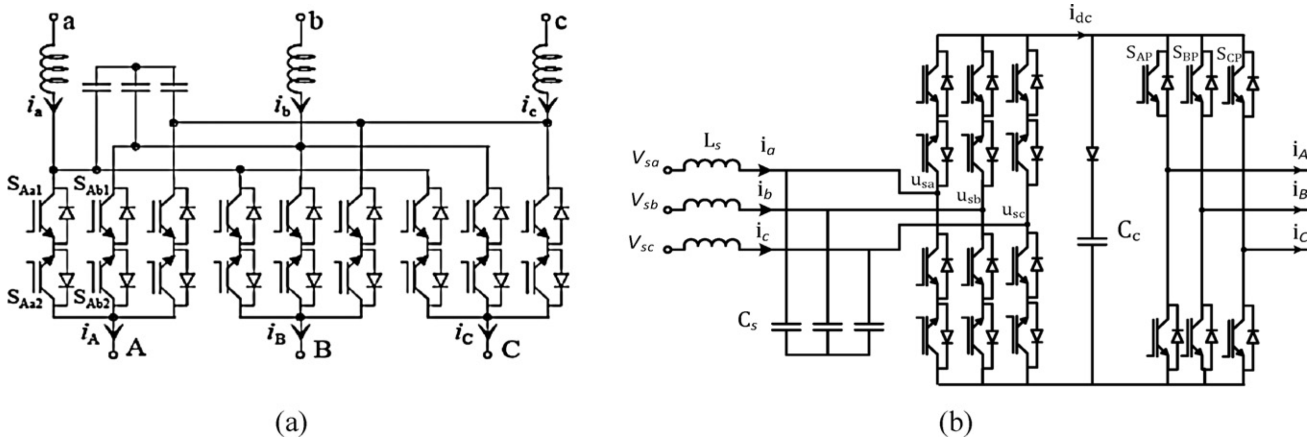

Fig. 1. Matrix converters: (a) direct and (b) indirect.

distortions. In [10] and [11], a boost converter is added to the matrix converter leading to improvement of voltage transfer ratio to unity. Despite using a very complicated control strategy in this solution, the input currents still contain large distortions and the integrity of the matrix converter, the salient advantage of matrix converter, has been lost because of insertion of many added components such as the boosting reactor and capacitor. In [12–16], other methods have been proposed to improve the voltage transfer ratio of the IMC, but input/output waveforms with low quality and lack of the integrity are the major defects of these methods too. Also, in [17] the IMC has been controlled in a reverse power mode in order to boost the input AC source voltage in distributed generation application.

After scrutinizing the functionality and switching strategy of traditional IMC in Section 2, the paper introduces the proposed IMC with the ability of boosting voltage and new switching strategy in Section 3. Throughout an analytical study given in Section 4, the paper proves that the proposed converter in its ideal form has an unlimited voltage transfer ratio (limited when considering parasitic elements), sinusoidal input/output currents with low distortion. In addition, unlike the previous research, the operation of the proposed converter is not based on any special control strategy which is an important feature in viewpoint of industrial applications. In Section 5 the idea is contrasted with other solutions and its advantages and disadvantages are investigated. Section 6 presents the simulation and experimental results to demonstrate and verify the marvelous performance of the proposed converter achieved without any close looped control.

2. Conventional indirect matrix converter

Before presenting of the new converter, conventional IMC is introduced to provide an analytical basis for describing the principles of the proposed converter. The basic concept of the IMC is to separate the AC/AC conversion into two stages, namely the line and load side stages without bulky DC-link capacitor as shown in Fig. 1(b). The line side converter is composed of six bidirectional switches possibly built with 12 unidirectional switches, while the load side one is a conventional inverter and has six unidirectional switches. As a result, independent switching modulation strategies can be applied to each stage. In addition, the clamp circuit is an important component for both direct and indirect matrix converters. Generally, the clamp circuit of a DMC consists of dual six-pack diode rectifiers and one capacitor. Also, as shown in Fig. 1(b) a much simpler clamp circuit consisting of only one diode and one capacitor at the DC-link can be used for IMCs. It should be noted that the appropriate value of the clamp capacitor depends on the load current, the load inductance, and the highest allowable capacitor voltage. However, this capacitor is very small in comparison with conventional back to back converters DC-link capacitor. The operation of the clamp circuit is as follows:

- When the converter is started, all the switches in the line side turn on initially and the clamp capacitor voltage is charged up to the maximum peak line voltage.
- Under normal operation, the clamp diode is reverse-biased and this clamp circuit does not operate.
- Under a fault state, all switches of the load side converter are turned off immediately and the energy stored in the inductive load flows into the clamp capacitor to avoid high voltage spikes and protect the power switches [5].

2.1. Switching strategy for the conventional IMC

Assuming the source voltages be described as:

$$\begin{aligned} V_{sa} &= V_{sm}\cos(\theta_a) \\ V_{sb} &= V_{sm}\cos(\theta_b) \\ V_{sc} &= V_{sm}\cos(\theta_c) \end{aligned} \tag{1}$$

where

$$\theta_a = \theta_{in}, \quad \theta_b = \theta_{in} - \frac{2\pi}{3}, \quad \theta_c = \theta_{in} + \frac{2\pi}{3} \tag{2}$$

And the input voltages of the line side converter be equal to those of supply for simplicity of analysis as follows:

$$U_{sa} \cong V_{sa}, \quad U_{sb} \cong V_{sb}, \quad U_{sc} \cong V_{sc} \tag{3}$$

The space vector PWM control method explained in [2] for an ensured safe commutation identifies six intervals based on detection of the angle of input voltages (see Fig. 2). During each interval, only one of the three input phase voltages has the largest magnitude (absolute value). For example, V_{sa} and V_{sc} have the largest magnitude during the intervals 1 and 2 respectively. The purpose of the line side converter is to draw sinusoidal currents at the input along with transferring the maximum available possible positive voltage (to act the function of rectifying) to the DC-link, by modulating between the two line-to-line input voltages [7].

Each switching cycle of the line side converter is split into two portions in order to benefit from the both largest positive line voltages at the input. In this way, the switching states of line side converter switches are fixed during each portion and the DC side voltage V_{dc} equals to one of the two largest positive line voltages. For instance, V_{sc} in interval 2 has the largest absolute voltage, as shown in Fig. 2, and the two largest positive line voltages are

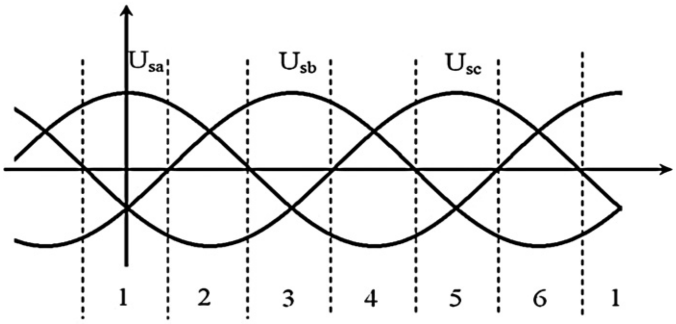

Fig. 2. Six intervals of a switching cycle.

Table 1
DC voltages in each interval.

Interval	Portion 1 V_{dc}	Portion 2 V_{dc}
1	$V_{sa} - V_{sb}$	$V_{sa} - V_{sc}$
2	$V_{sb} - V_{sc}$	$V_{sa} - V_{sc}$
3	$V_{sb} - V_{sc}$	$V_{sb} - V_{sa}$
4	$V_{sc} - V_{sa}$	$V_{sb} - V_{sa}$
5	$V_{sc} - V_{sa}$	$V_{sc} - V_{sb}$
6	$V_{sa} - V_{sb}$	$V_{sc} - V_{sb}$

$V_{sa} - V_{sc}$ and $V_{sb} - V_{sc}$ respectively. Within each portion, one of these line voltages is transferred to DC-link terminal. Table 1 elaborates the DC voltage during the two portions of switching cycle for all six intervals. Now the function of the load side converter can be considered as an equivalent DC/AC inverter with different DC voltages during different portions.

In order to draw sinusoidal input currents the duty ratio of the switched input voltages should be appropriately selected. According to the space vector modulation (SVM) the duty ratio of the adjacent active input current vectors (see Fig. 3) in a current source rectification stage (d_γ and d_δ) can be expressed as:

$$d_\gamma = m_i \times \sin\left(\frac{\pi}{3} - \theta_{in}\right), \quad d_\delta = m_i \times \sin(\theta_{in}) \tag{4}$$

where m_i is the rectification stage modulation index and θ_{in} is the angles of the input current reference vectors.

The sum of duty ratios of the line side converter is:

$$d_\gamma + d_\delta < 1 \tag{5}$$

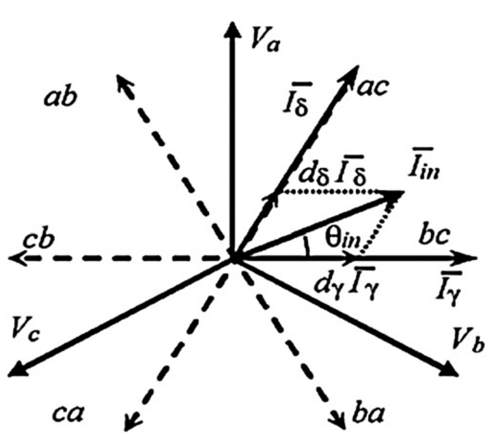

Fig. 3. Generation of the current reference vectors using space vector modulation for line side converter.

According to SVM the duration of the zero vector completes the switching period as:

$$d_0 = 1 - (d_\gamma + d_\delta) \tag{6}$$

In the rectifier stage, the modulation index m_i is set to unity to achieve maximum attainable voltage in the DC-link. However, the zero vectors in the rectifier stage will reduce the local-averaged DC-link voltage, by making the DC-link voltage zero. Moreover, the zero vectors lead to abrupt voltage fluctuation from line-to-line voltage to zero in the DC-link, which may cause potential hazard in the semiconductor breakdown. Thus, in all research in the field of indirect matrix converter the zero vectors have been eliminated in rectification stage as follows [4,5]:

Supposing that in interval 2 phases a and b are positive, phase c is then negative. One can derive:

$$\left|V_{sc}\right| = \left|V_{sa}\right| + \left|V_{sb}\right| \tag{7}$$

In portion 1 the DC voltage is equal to V_{ac} and positive. The duty ratio of this portion is selected as:

$$d_{ac} = -m_i \frac{\cos(\theta_a)}{\cos(\theta_c)} \tag{8}$$

In portion 2 the DC voltage is equal to V_{bc} and positive. The duty ratio of this portion is selected as:

$$d_{bc} = -m_i \frac{\cos(\theta_b)}{\cos(\theta_c)} \tag{9}$$

If the rectifier stage modulation index m_i is set to unity, it yields:

$$d_{bc} + d_{ac} = 1 \tag{10}$$

And the average DC side voltage in this switching cycle becomes:

$$V_{dc} = d_{bc} \times (V_{sb} - V_{sc}) + d_{ac} \times (V_{sa} - V_{sc}) \tag{11}$$

Substituting (1), (3), and (4) in (11), one can finally obtain:

$$V_{dc} = \frac{3 \times V_{sm}}{2 \times \left|\cos(\theta)\right|} \tag{12}$$

where $\cos(\theta) = \max\{\cos(\theta_a), \cos(\theta_b), \cos(\theta_c)\}$.

Fig. 4 shows the DC-link voltage and Fig. 5 depicts its enlarged illustration for the two mentioned intervals during one switching cycle.

In each portion the IMC can be considered as a conventional inverter with different DC-link voltage. Now, output voltages with desired frequency and amplitude can be generated through the space vector PWM modulation of the load side converter. Fig. 6 shows the DC-link voltage during one switching period. The switching sequence of the load side converter along with the gating signal of one switches (S_{AP} in Fig. 1(b)) are illustrated in Fig. 6. It can be seen that a symmetric (double edge) switching sequence is used for each portion. Synchronization of the line and load side converters beside a selection of duty ratio of portions according to the input phase voltages lead to sinusoidal input and output currents [4].

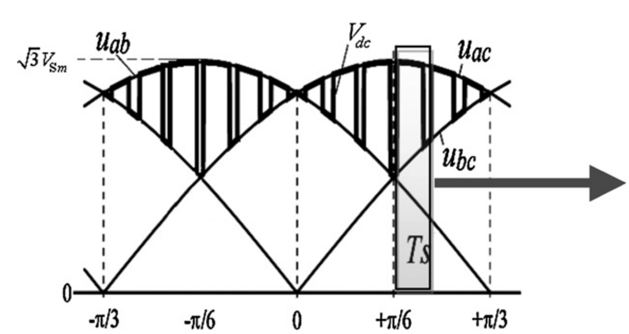

Fig. 4. Input line and DC-link voltages.

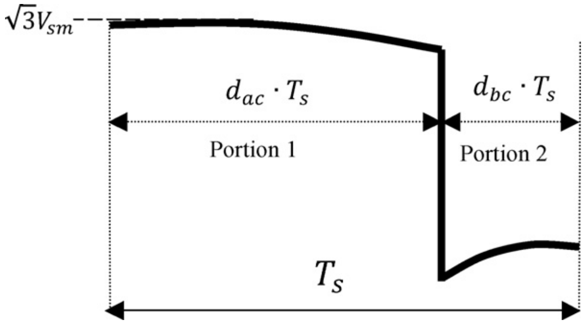

Fig. 5. DC-link voltage during one switching cycle.

3. Proposed indirect matrix converter

3.1. Proposed converter power circuit

The power circuit of the proposed IMC consisting of one line side converter, the clamp circuit and the load side converter is shown in Fig. 7. Comparing the converters of Figs. 1(b) and 7, it can be seen that:

(1) The only difference between the conventional IMC and the proposed one is four additional unidirectional switches (S1, S2, S3 and S4).
(2) No additional capacitor or inductor is added at the DC-link, thus the integrity of the converter has been kept.
(3) While load sides of the both converters are similar, the proposed IMC has 3 additional inputs.

3.2. AC–AC voltage boosting principles

Elaboration of operation principles of the proposed converter can be simply understood from the principles of an AC–AC boost chopper shown in Fig. 8.

While the output AC voltage, Vo, will be controlled by a PWM signal controlling the switches of circuit in a complementary manner, the process produces a chopped output voltage consisting of a fundamental component and switching frequency harmonics. These harmonics can be filtered out by a low pass filter. The basic concept of this circuit is explored directly from its well-known DC/DC counterpart. The only difference is the existence of bidirectional switches which is because of alternative currents. As with DC/DC boost converters, when S1 is turned on the source supplies energy to inductor for a period of time $D_{on}\,T_s$ where D_{on} is the duty ratio of switch and T_s is the switching period. For the remaining time of switching period, $(1 - D_{on}) \times T_s$ seconds bidirectional switches are conducting the stored energy to the load. Fig. 9 shows the input current, input voltage and output voltage of the converter.

Using the small ripple approximation for the output voltage in steady state it yields [18]:

$$V_o = \frac{V_s}{1 - D_{on}} \tag{13}$$

where V_s and V_o are the input and output voltages respectively. From Fig. 9(a) and (b), it can be seen that output voltage can be boosted up.

3.3. Operation principles of the proposed converter

The main idea for improving the voltage transfer ratio of the conventional IMC is to add the AC–AC voltage boosting function, discussed in previous section, to the line side converter in order to increase the input voltage of the converter (U_{sa}, U_{sb} and U_{sc}) greater than the supply voltage (U_{sa}, U_{sb} and U_{sc}) in a similar way. For this purpose three additional switches are added with anti-parallel diodes for disconnecting the input filter capacitors when the input inductors in charging state through the supplied voltages and the switches of line side converter. Since the line side converter should now serve to achieve not only sinusoidal unity power factor phase currents but also boosted line voltages at the input, its switching strategy should be modified as well.

Considering the load side converter as a current source for simplicity and the supply voltage U_{sa}, U_{sb} and U_{sc}, in the interval 2 of Fig. 2. The proposed four steps switching sequence of the line side converter during a switching period can be explained as follows:

(1) As shown in Fig. 10(a), the switches S_1, S_2 and S_3 are on and transfer the converter input line voltage $U_{sa} - U_{sc}$ to the DC-link in analogy to conventional switching strategy of the IMC. In this condition the clamp diode turns on and the clamp capacitor C_c starts charging.

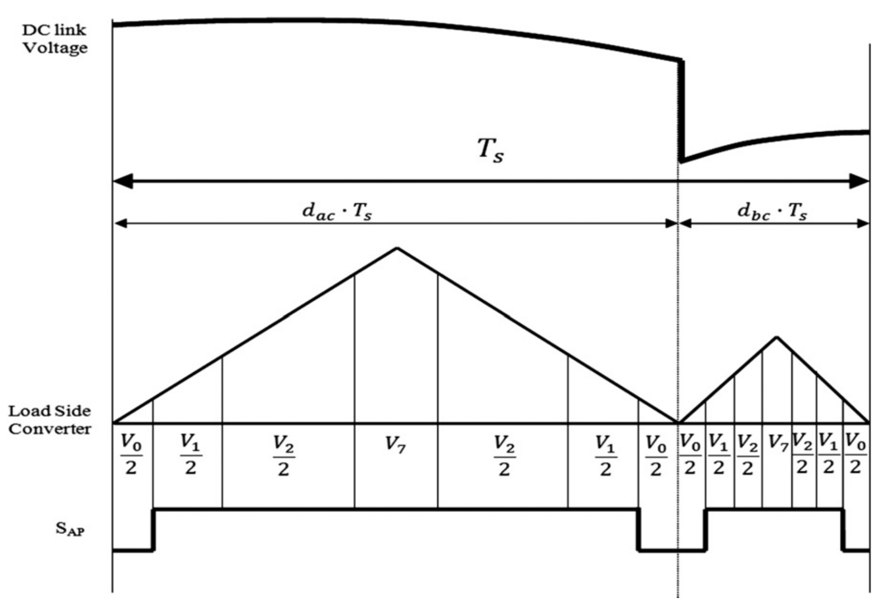

Fig. 6. PWM sequence of the load side converter.

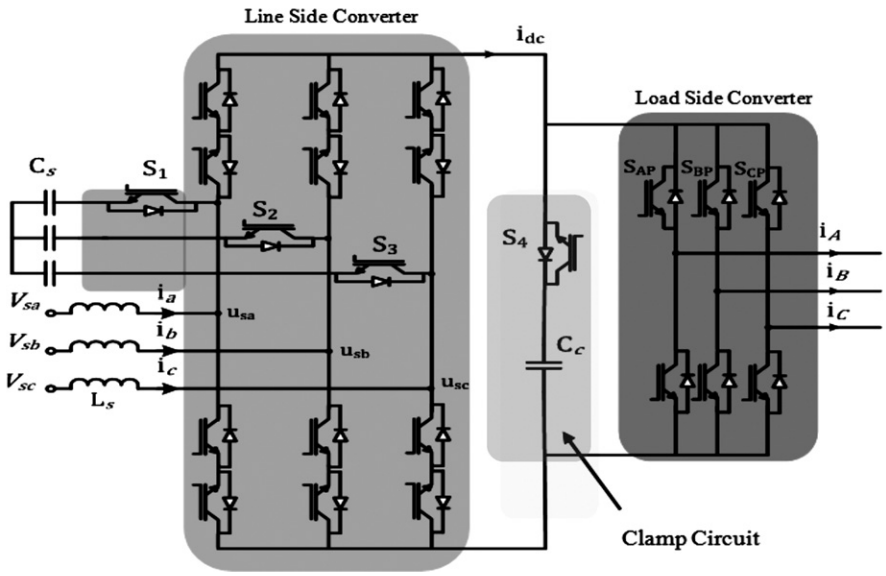

Fig. 7. Proposed IMC.

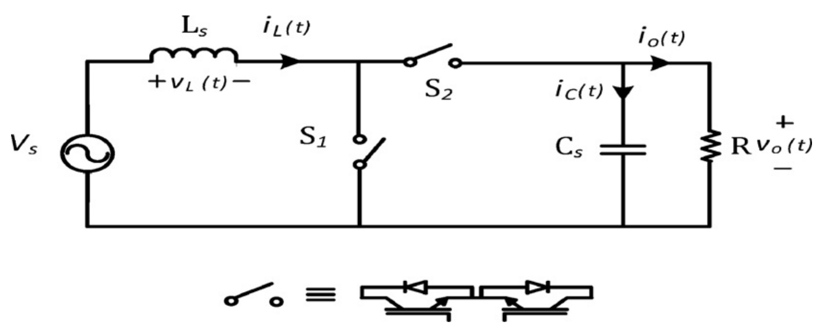

Fig. 8. AC/AC boost chopper.

(2) As shown in Fig. 10(b), after the clamp capacitor C_c is charged to the peak of the input line voltage ($\sqrt{3} \times U_{sm}$) the clamp circuit diode turns off. In this step the DC-link voltage is equal to U_{ac}.
(3) Assume that the line side converter modulation index m_i be lower than 1:

$$m_i < 1 \tag{14}$$

Thus, based on (8), (9) and (14) the sum of duty ratios is:

$$d_{ac} + d_{bc} = -m_i \frac{\cos(\theta_a)}{\cos(\theta_c)} - m_i \frac{\cos(\theta_b)}{\cos(\theta_c)} \tag{15}$$

From (6), (10) and (15) with $m_i < 1$ the zero duty ratio d_0 is equal to:

$$d_0 = 1 - m_i \tag{16}$$

Assume that in $d_0.T_s$ portion of switching period, all upper bidirectional switches of the line side converter are switched on and the switches S_1, S_2 and S_3 are switched off and S_4 is switched on. Thus, in this duration the input filter inductors are charged to perform required boosting function, the input filter capacitors remain at the previous voltage level and the load side converter is fed by the clamp capacitor (charged in step one). Fig. 10(c)

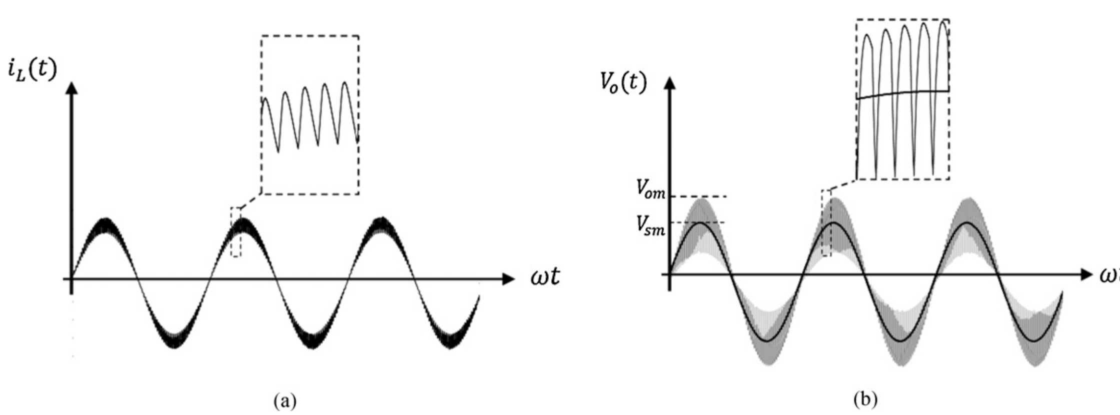

Fig. 9. AC/AC boost chopper: (a) input current and (b) input/output voltage.

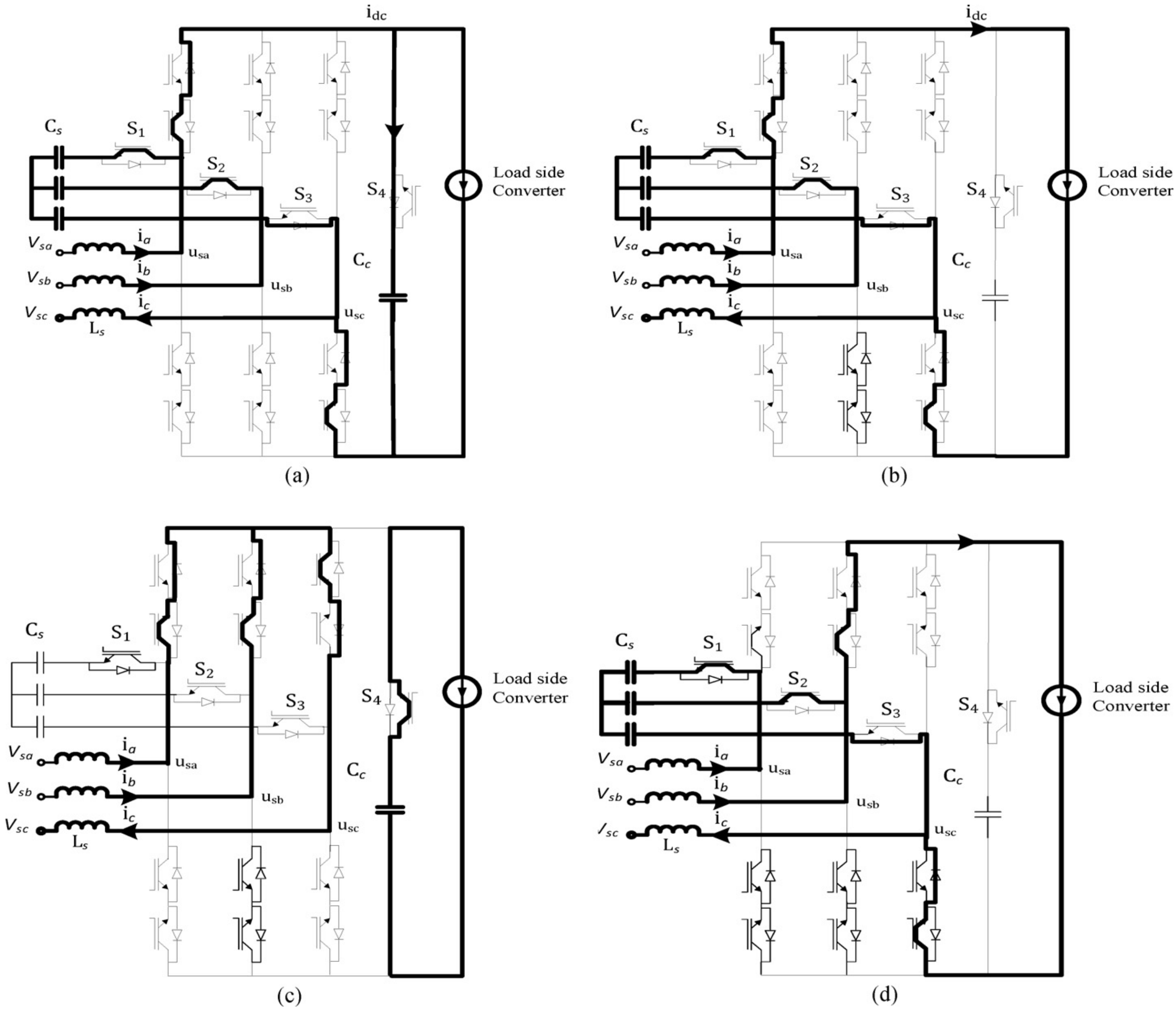

Fig. 10. Switching strategy of the line side converter in step (a) one, (b) two, (c) three, and (d) four.

shows the power circuit in this step. In this step the DC-link voltage is equal to V_{Cc}.

(4) As shown in Fig. 10(d), in this step the switches S_1, S_2 and S_3 are switched on, S_4 is switched off while the line voltage, $U_{sb} - U_{sc}$ is transferred to DC-link in analogy to conventional switching strategy of the IMC. Thus, the boosting energy stored in the filter inductors is released to the filter capacitors resulting in an amplified voltage at the input. In this step the DC-link voltage is equal to U_{bc}.

4. Analyses of the proposed IMC

4.1. DC-link voltage

Exploring the similarity of principles of boosting voltage for the proposed converter and those elaborated for AC/AC boosting chopper of Fig. 8, one can find the duty ratio of zero vector of the line side converter to be:

$$d_0 = 1 - m_i = D_{on} \Rightarrow 1 - D_{on} = m_i \tag{17}$$

Thus, from (13) the converter input voltages are:

$$U_{sa} = \frac{V_{sa}}{m_i} \tag{18a}$$

$$U_{sb} = \frac{V_{sb}}{m_i} \tag{18b}$$

$$U_{sc} = \frac{V_{sc}}{m_i} \tag{18c}$$

As indicated by (18), the input voltage can become far greater than the supplied voltage while the line side converter modulation index is less than unity $m_i < 1$. Therefore, the peak value of DC-link voltage can now reach the value $\sqrt{3} \times V_{sm}/m_i$ with is boosted as much as of $1/m_i$ when compared with the corresponding value $\sqrt{3} \times V_{sm}$ in a conventional IMC. This is also depicted in Fig. 11.

Fig. 11 shows the DC-link voltage of the proposed converter during one switching cycle.

From Fig. 11 the average value of the DC-link voltage can be expressed as:

$$V_{dc} = m_i \times d_{bc} \times (V_{sb} - V_{sc}) + d_{ac} \times (V_{sa} - V_{sc}) + (1 - m_i) \times V_{Cc} \tag{19a}$$

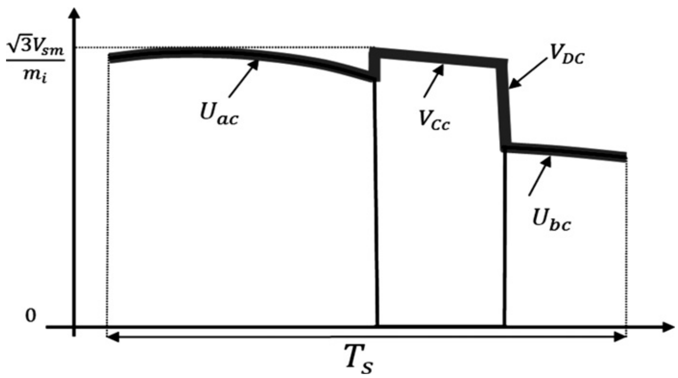

Fig. 11. DC-link voltage during one switching period.

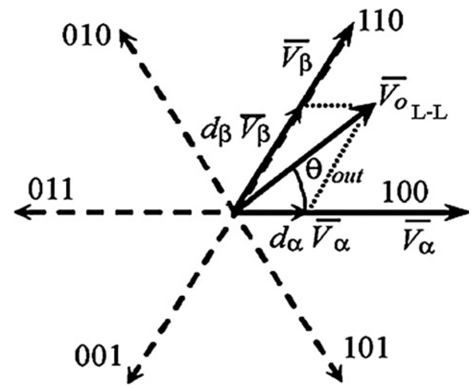

Fig. 13. Generation of the reference vectors using space vector modulation for the load side converter.

$$V_{dc} = m_i \times \left\{ \frac{\cos(\theta_b)}{\cos(\theta_c)} \times \left(\frac{V_{sm}\cos(\theta_b) - V_{sm}\cos(\theta_c)}{m_i} \right) + \frac{\cos(\theta_a)}{\cos(\theta_c)} \times \left(\frac{V_{sm}\cos(\theta_a) - V_{sm}\cos(\theta_c)}{m_i} \right) \right\} + (1 - m_i) \times \frac{\sqrt{3}V_{sm}}{m_i} \tag{19b}$$

From (11) and (12), (19b) can be simplified to:

$$V_{dc} = \frac{3 \times V_{sm}}{2 \times |\cos(\theta)|} + (1 - m_i) \times \frac{\sqrt{3}V_{sm}}{m_i} \tag{20}$$

It should be noted that the small discharge of the clamp capacitor during step 3 has been neglected for simplicity.

From (12) and (20), it can be seen that the DC average value of DC-link voltage of the proposed IMC has a new term being controlled by the modulation index m_i. Fig. 12 shows the DC-link voltage versus the line side converter modulation index.

4.2. Voltage transfer ratio of the proposed converter

As shown in Fig. 13 it is possible to derive for an average output line-to-line vector $\bar{V}_{oL-L}$ in one switching cycle by vector algebra [19]:

$$\bar{V}_{oL-L} = d_\alpha \times \bar{V}_\alpha + d_\beta \times \bar{V}_\beta \tag{21}$$

where d_α and d_β are duty ratios of the adjacent voltage vectors and can be found by:

$$d_\alpha = \frac{\bar{V}_{oL-L}}{V_{dc}} \times \sin\left(\frac{\pi}{3} - \theta_{out}\right) \tag{22a}$$

$$d_\beta = \frac{\bar{V}_{oL-L}}{V_{dc}} \times \sin(\theta_{out}) \tag{22b}$$

The maximum available voltage ratio $\bar{V}_{oL-L}/V_{dc}$ in linear modulation is unity in (22a) and (22b). Substituting (12) into (22a) and (22b) results in the maximum output line to line voltage to input voltage for conventional IMC and yields:

$$\frac{|\bar{V}_{oL-L}|}{V_{sm}} = \frac{3}{2} \tag{23}$$

Since $\bar{V}_{oL-L} = \sqrt{3}V_{om}$, the conventional IMC maximum transfer ratio equals to:

$$\frac{V_{om}}{V_{sm}} = \frac{\sqrt{3}}{2} = 0.866 \tag{24}$$

Substituting (20) into (22a) and (22b) leads to an expression for the maximum output line to line voltage to input voltage for the proposed IMC and yields:

$$\frac{|\bar{V}_{oL-L}|}{V_{sm}} = \frac{3}{2} + (1 - m_i) \times \frac{\sqrt{3}}{m_i} \tag{25}$$

And the proposed IMC transfer ratio equals to:

$$\frac{V_{om}}{V_{sm}} = \frac{\sqrt{3}}{2} + (1 - m_i) \times \frac{1}{m_i} \tag{26}$$

which is obviously adjustable by the line side converter modulation index, m_i. Fig. 14 shows the variation of the voltage transfer ratio versus m_i for the proposed IMC:

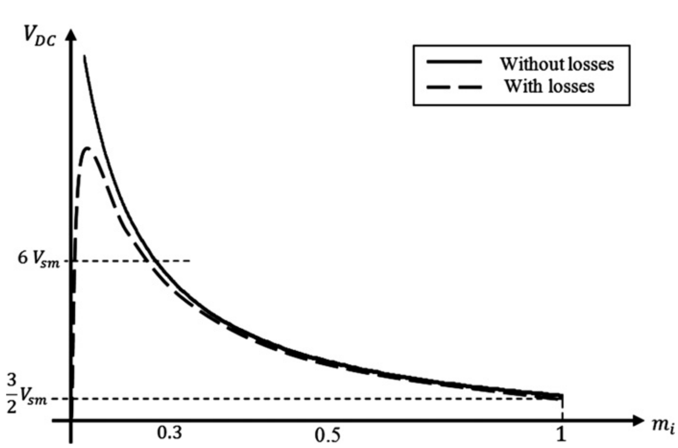

Fig. 12. DC-link voltage versus line side converter modulation index.

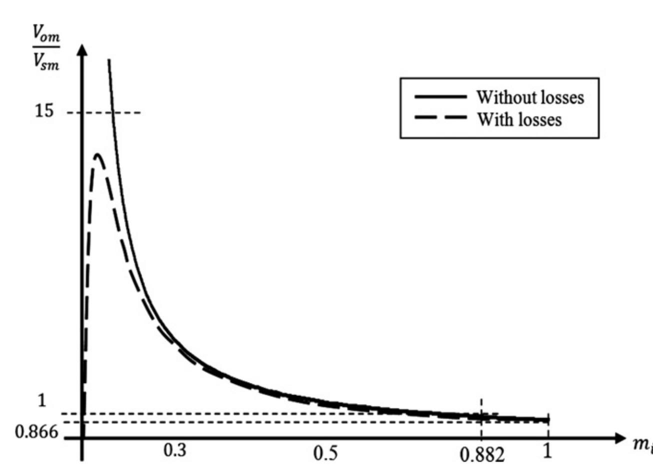

Fig. 14. Voltage transfer ratio of the proposed converter versus line side converter modulation index.

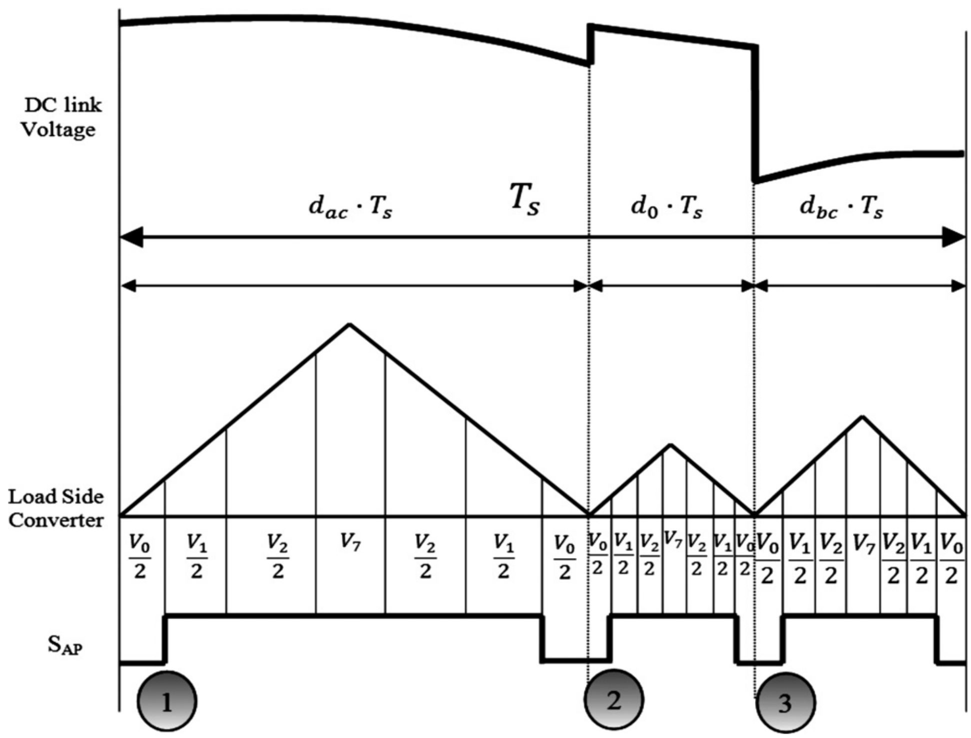

Fig. 15. Switching sequence of the proposed IMC.

Considering all the components as ideal, Fig. 14 depicts that the voltage transfer ratio of the proposed IMC can be infinitely controlled with line side converter modulation index. But in a real circuit because of the parasitic components of switches, conductor resistances, output/input capacitances and etc. boosting function is limited same as any other boost circuit.

4.3. Improved switching strategy

As previously discussed in Section 2, a proper sequence consisting of two sets of space voltage vectors should be used in each portion of the DC-link voltage during one switching period in order to synchronize the line and load side converters in a conventional IMC (Fig. 6) [5]. This imposes a twofold higher switching frequency for the load side converter. In case of proposed IMC, the DC-link voltage has three portions, as shown in Fig. 11, and therefore three sets of space voltage vectors are needed to fulfill the synchronization conditions according to the previous strategy. Fig. 15 illustrates this problem. It is obvious that the load side converter switch (S_{AP}) has three transitions during each switching period resulting in a threefold switching frequency of the load side converter which is very disadvantageous. In [20] the authors proposed a new sawtooth switching strategy reducing the switching frequency of the load side converter of a conventional IMC to half. Fig. 16 shows the sawtooth switching strategy for the proposed converter and the resulted switching signal. It can be seen that the number of switching transitions of the load side converter reduced to one third resulting in lower switching frequency and switching losses. In addition, in [20] it is shown that the sawtooth strategy has good performance in viewpoint of input/output waveforms total harmonic distortions (THD).

From Fig. 16, it can be seen that the applied DC-link voltage for vector V_2 changes for a short period of time (hashed regions). This voltage variation appears in output voltages/currents as some distortions. But since at unity voltage transfer ratio the hashed region is too short (10% of duty cycle of the vector V_2 in worst case) the distortions are expected to be low and negligible.

4.4. Modified clamp circuit

As discussed in Section 2, direct conversion needs a small energy storage device for preventing overvoltage in fault conditions. One of still remaining problems of clamp circuit of matrix converters (specially Fig. 1(b)) is that once the clamp capacitor is charged (after a fault condition), there is no way for discharging it before next restart and mounting a discharge circuit is unavoidable. However, In case of the proposed IMC, since the clamp capacitor continuously exchanges its energy with the load in normal operation, after next restart the excess charge of the clamp capacitor is discharged in few switching periods into the load and its voltage gets back to the normal operating level. Thus, there is no need for an extra discharging circuit.

5. Comparison with other solutions

As mentioned in Section 1, some solutions have been already proposed for improving the IMCs voltage transfer ratio from 0.866 to 1. All of these solutions can be categorized in two groups:

5.1. Control/switching strategy modification

These modifications include modifying the control strategy or switching pattern of the IMC without adding any power component to the IMC in order to keep the cost, integrity and efficiency of the converter. In [9] and [12] the IMC operates in overmodulation region in order to increase the voltage transfer ratio of the converter. In other words, the load side converter of the IMC generates the output voltage with greater amplitude in this region. But, in this region the output voltage and currents contain low order harmonics and large distortions. In [17] a control strategy has been proposed to control the IMC in a reverse power mode for distributed generation. The idea behind it is the fact that, since the IMC voltage transfer ratio is equal to 0.866 in forward power direction and it works as a buck converter, as shown in [17], if the IMC can be controlled in reverse direction, the voltage gain would be equal to 1.15

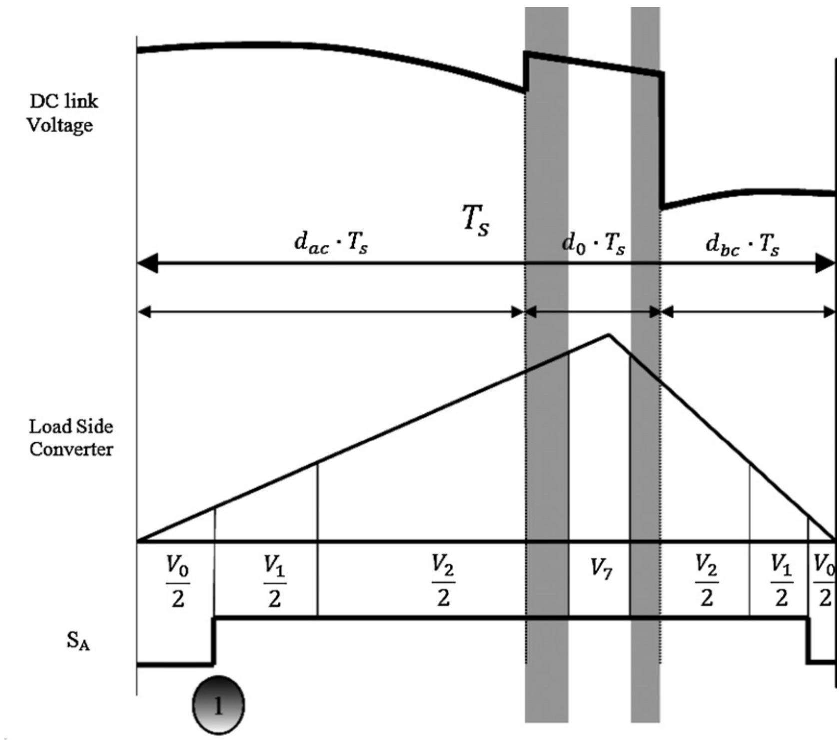

Fig. 16. PWM sequence of the proposed IMC with sawtooth switching strategy.

(1/0.866) and it can be considered as a boost converter. Although this is an interesting solution, but there are two disadvantages with this method:

(1) The IMC cannot be used as a bidirectional power flow converter.
(2) The input AC source should have voltage with smaller amplitude respect to grid voltage.

These operation circumstances and limitations restrict the application of this technique to distributed generation applications.

5.2. Combined control/switching and topology modifications

These solutions modify both the control strategies (and switching pattern) and power topology of the converter in order to add boost function to the IMC and to improve its voltage transfer ratio. Consequently, keeping the cost, integrity and the efficiency of the IMC should be considered as affected factors. In [10] and [11], a boost converter with additional power switches and reactive elements has been added at the DC-link. Thus, the integrity of the IMC has been lost and the efficiency of the converter decreases. Also,

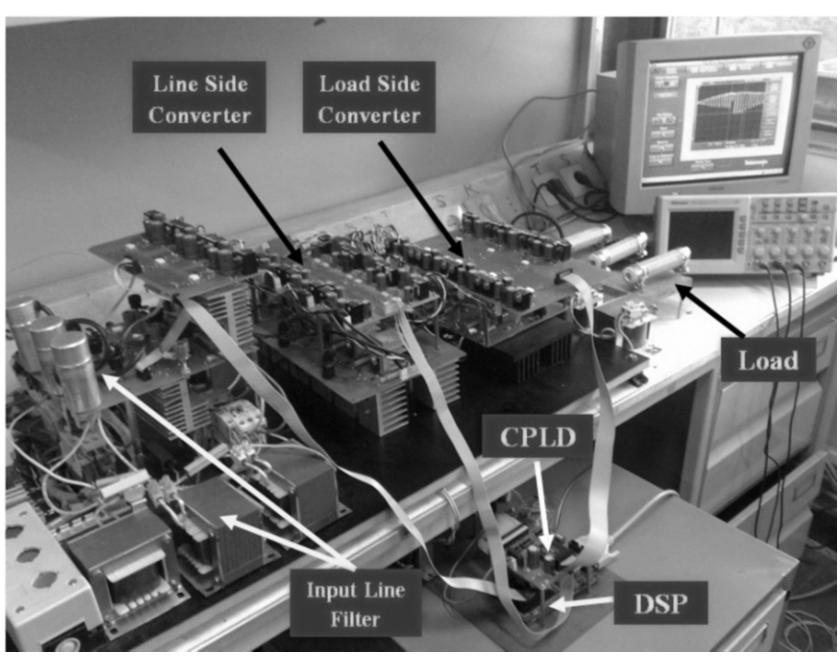

Fig. 17. The prototype of the proposed converter.

despite using a very complicated control strategy the quality of the input currents is very poor.

In [15] Z-source network is added to the DC-link of a conventional IMC oriented in the direction of forward power flow and boost functionality is added. However, besides more costly passive components the integrity of the converter has been lost.

As shown in previous sections, the solution proposed in this paper modifies both the converter topology and its switching pattern. The following advantages and disadvantages can be counted for this method:

- Advantages:
  - Only four additional low power switches have been added to the IMC and no additional reactive elements have been introduced to the DC-link. Thus, the integrity of the IMC has been kept.
  - The operation of proposed IMC does not need any control strategy to keep the voltage transfer ratio of the IMC unity.
  - As shown in Section 6, the quality of the input and output currents meets the IEC 61000-3-2 [21] requirements.
  - The ability of bidirectional power flow is preserved.
- Disadvantage:
  - The four added low power switches slightly decreases the efficiency of the proposed IMC when compared to the conventional IMC. However, as discussed in Section 3.3, these switches just carry the reactive charging/discharging current of input filter capacitances with an effective value much smaller than the effective value of the load current flowing through other switches. Especially the switch S4 conducts for the short duration of $(1 - m_i)$ T_s within the switching cycle. Actually, the 4 added switches are low power making their integration into the power chip very possible. Hence, they do not affect the converter efficiency seriously. Also, it is worth noting that a conventional IMC with a slightly higher efficiency provides a voltage transfer ratio even lower than 0.866 in the field of experiments resulting in restriction of its applications and industry adaption.

6. Simulation and experimental verifications

In order to evaluate the operation of the proposed converter a 5 kW converter, as shown in Fig. 7, has been simulated in Matlab/Simulink. Furthermore a 5 kW laboratory prototype (Fig. 17) has been built up to verify the simulation results. Table 2 describes the parameters of experimental set-up and simulated converter:

The converter switches are 1200 V, 40 A IGBT from Infineon and controlled by a processor system consisting of a 16-bit fixed point DSP board (TMS320F2812-ezdsp) and a functional digital logics

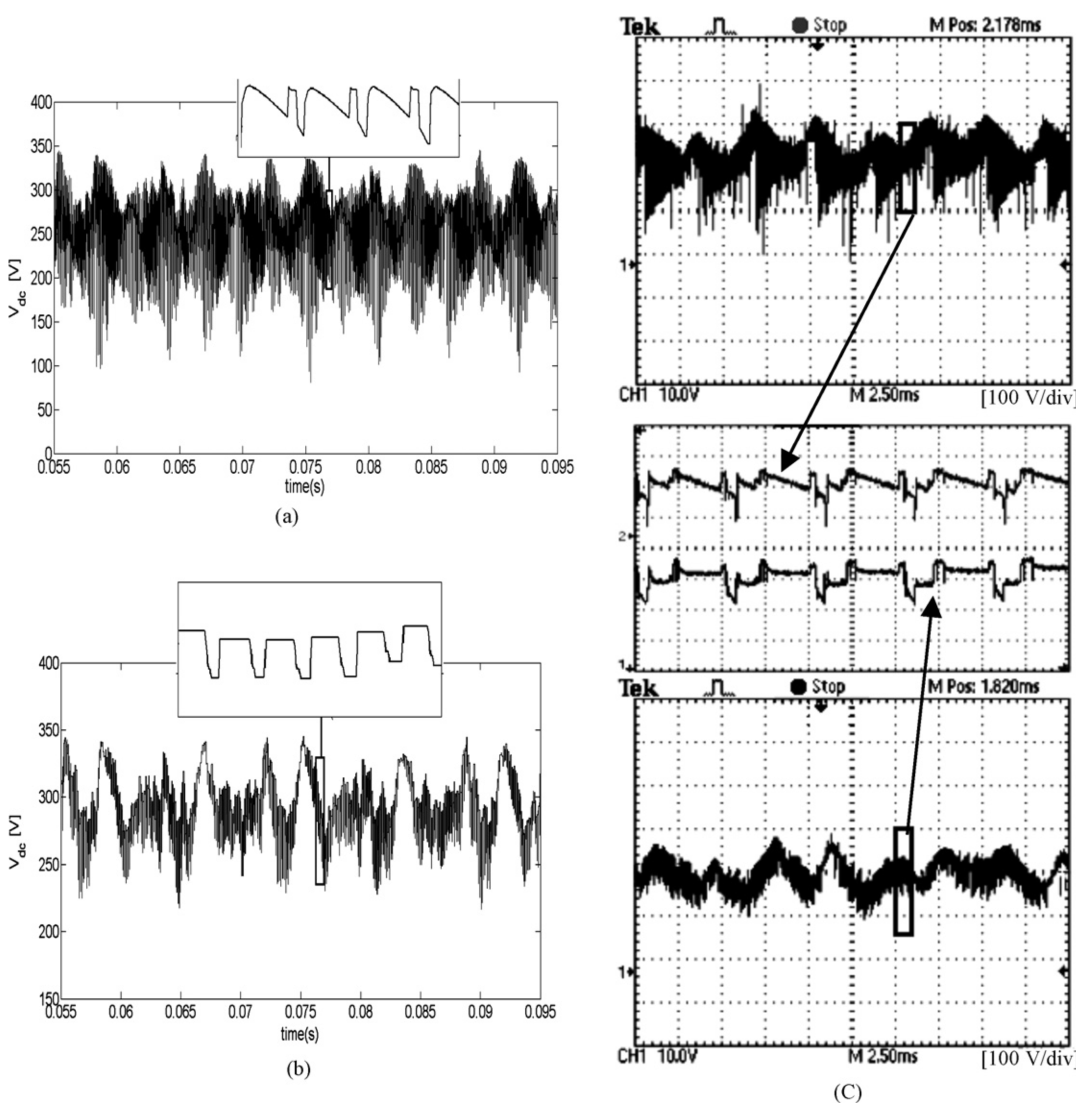

Fig. 18. (a) DC-link voltage (simulation results), (b) clamp capacitor voltage (simulation results), and (c) DC-link voltage (top) and clamp capacitor voltage (bottom) (experimental results).

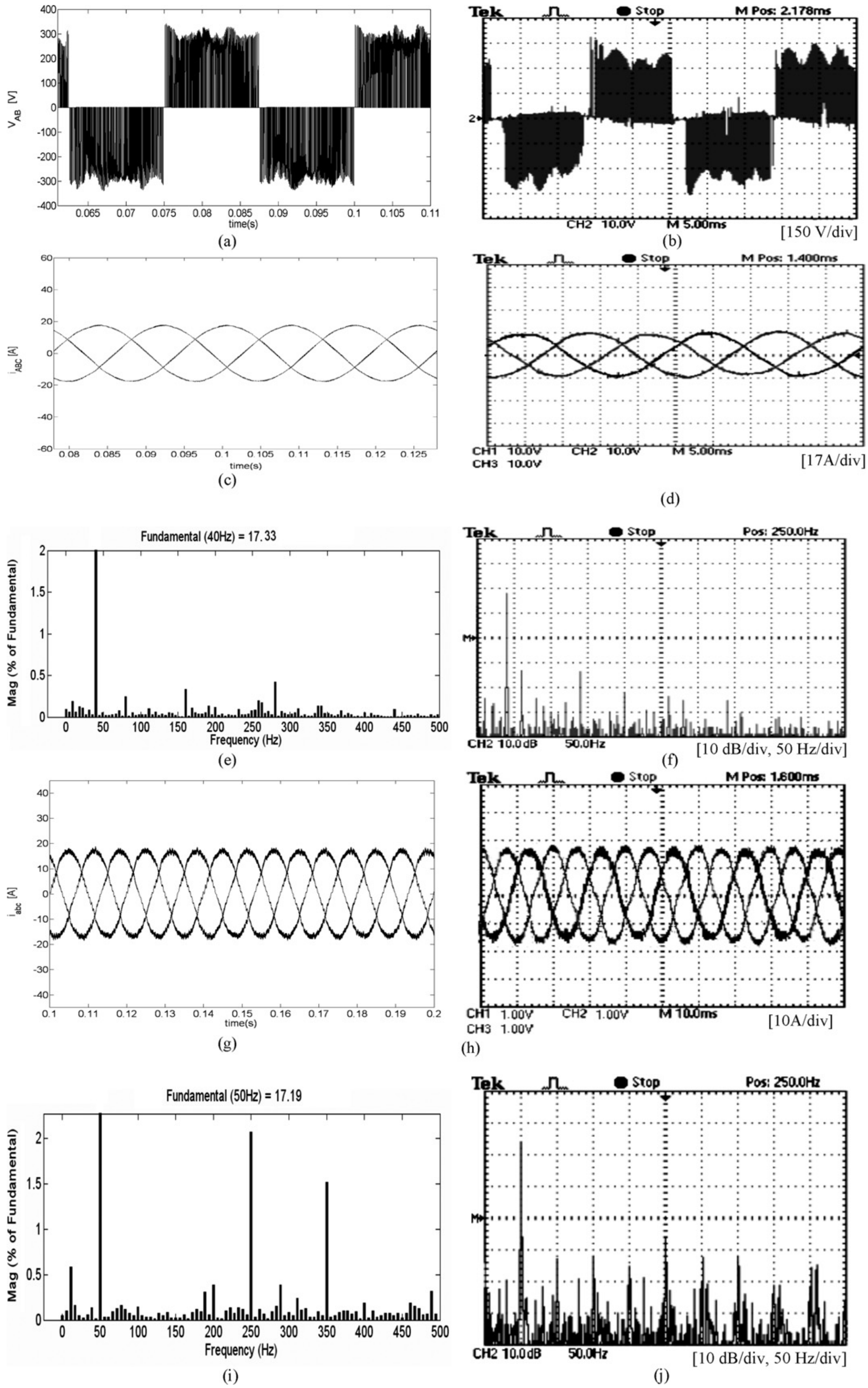

Fig. 19. Simulation (left) and experimental (right) waveforms of (a) and (b) output line voltage, (c) and (d) output currents, (e) and (f) spectrum of output currents, (g) and (h) input currents, (i) and (j) spectrum of input currents under unity voltage transfer ratio.

Table 2
Proposed converter data.

IMC parameters	
Input line voltage, V_{sa}	220 V
Fundamental supply frequency, F_i	50 Hz
Fundamental output frequency, F_o	40 Hz
Switching frequency, F_{sw}	10 kHz
Input filter inductance, L_s	700 μH
Input filter capacitance, C_s	5 μF
Clamp capacitor, C_c	5 μF
Load inductance, L_L	5 mH
Load resistance, R_L	8 Ω

programmed in Altera (EPM7128s). The network input voltage in all performed tests is distorted with low order harmonics 3rd, 5th and 7th and also 2% unbalance.

As discussed in many research papers, any type of disturbance in input line voltage is reflected directly to the load side in matrix converters. Thus, the experimental results in next sections can be better if a fully sinusoidal voltage source without any distortion is used. It is worthy to note that the operation of the converter is based on the proposed switching pattern and is quite without using any open/closed loop controller.

6.1. Evaluation of boosting function

In order to have a unity voltage transfer ratio, the modulation index of the line side converter has been set to 0.87 in both simulation and experiment tests based on depicted curve shown in Fig. 14.

Fig. 18 shows the DC-link (V_{dc}) and clamp capacitor (V_{Cc}) voltages of the proposed converter. Also as shown in zoomed areas of Fig. 18, the analyzed three segment DC-link voltage in Section 4.1 has been substantiated in both simulation and experiment tests.

Table 3
Conventional and proposed IMC input/output performance.

		Input current THD%	Output current THD%
Digital simulation	Conventional IMC	2	0.52
	Proposed IMC	3	0.63
Experiment test	Conventional IMC	2.3	1.42
	Proposed IMC	3.2	1.83

6.2. Input and output performance evaluation

Fig. 19 illustrates the simulation results (left column) and experimental results (right columns) of the proposed IMC under unity voltage transfer ratio. Fig. 19(a) and (b) shows the output line voltage (V_{AB}), (c) and (d) shows the output currents (i_{ABC}), (e) and (f) shows their associated spectrums, (g) and (h) shows the input currents (i_{ABC}), and (i) and (j) shows their associated spectrums under unity voltage transfer ratio. A good agreement can be seen between the practical and the simulation results given in Fig. 19.

Besides the high quality and sinusoidal input/output currents achieved without using any open/close loop control, Fig. 19(c) and (g) reveals that the fundamental amplitude of the input and output currents, being 17.33 A and 17.19 A, are close to each other confirming that the voltage transfer ratio of the converter is unity now.

Table 3 elaborates the THD of the input and output currents for both a conventional and the proposed IMC. From this table one can easily find that although in comparison to a conventional converter (with 0.866 voltage transfer ratio) the proposed IMC (with unity voltage transfer ratio) has input/output currents with slightly higher distortions, as expected, the THD of its input/output waveforms meets the IEC 61000-3-2 standard requirements very well even under a distorted supply voltage.

Fig. 20(a) and (b) shows the input and output currents of the IMC when the modulation index of the line side converter is set to 1. It

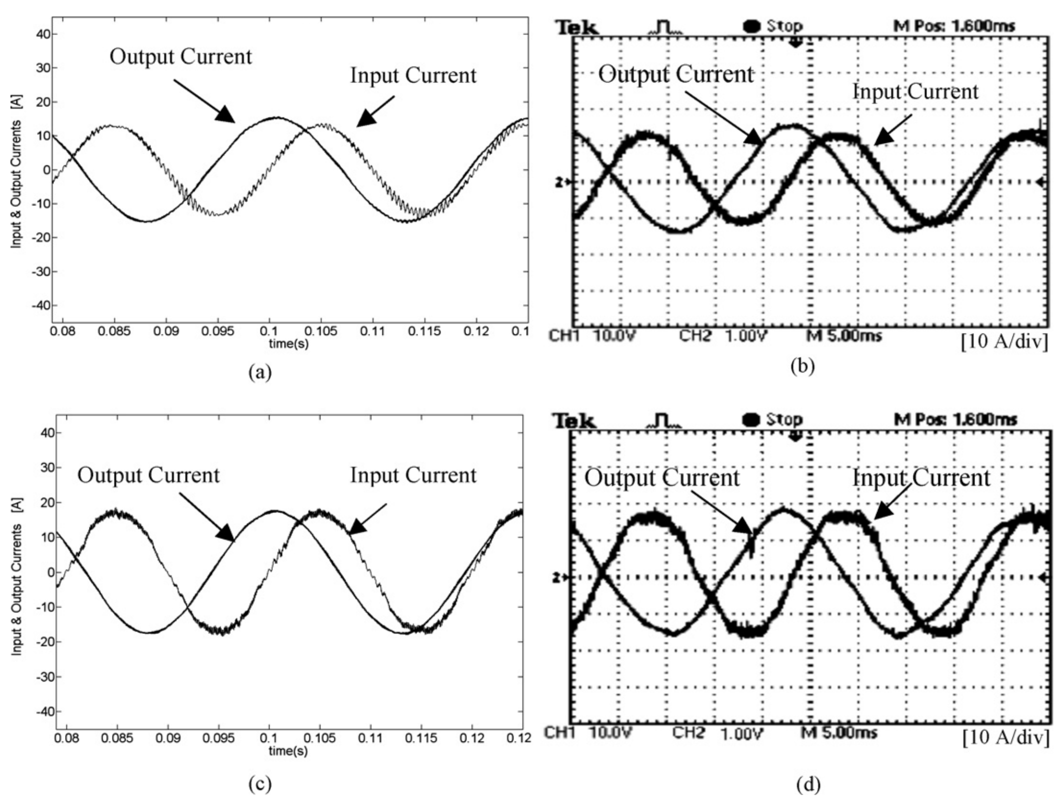

Fig. 20. Simulation (left) and experimental (right) waveforms of (a) and (b) input and output currents when $m_i = 1$ and (c) and (d) input and output currents when $m_i = 0.87$.

can be easily seen that the output current is larger than the input one in both simulation and experiment results. In this situation the voltage transfer ratio of the converter is 0.866. Fig. 20(c) and (d) shows the same currents when the modulation index of the line side converter is set to 0.87. It can be seen that the amplitude of the input and output currents are equal in this situation and therefore the voltage transfer voltage of the converter is unity now.

7. Conclusion

The paper proposes a practical solution for overcoming the voltage transfer ratio limitation in indirect matrix converters so that the advantages of this kind of AC–AC conversion can be still kept. Originating from the idea of AC boosting function, a perfection is brought to the conventional IMC topology with adding four unidirectional switches. A new switching strategy is applied to achieve the boosting function and to reduce the switching losses as well. While analyzing the boosting operation of converter, design equations are also explored that an unlimited voltage transfer ratio can be theoretically achieved. Besides the simulation results, excellent agreement of experimental certifies the ability of voltage boosting in the proposed IMC. Comparing the THD of input/output voltages and currents of the converter using the spectrum of simulation and experimental waveforms, the paper presents that the quality of both input and output quantities meet the IEC requirements under the unity voltage transfer ratio even without applying any open or closed loop control and under the disturbed supply voltage. As the functionality of voltage boosting and good performances of proposed IMC has been fully tested with simulation and a 5 kW prototype while keeping its integrity, the proposed converter can be an appropriate candidate for future AC–AC power conversion.

References

[1] J.W. Kolar, T. Friedli, J. Rodriguez, P.W. Wheeler, Review of three-phase PWM AC–AC converter topologies, IEEE Transactions on Industrial Electronics 58 (10) (2011) 4988–5006.
[2] M. Muroya, K. Shinohara, K. Iimori, H. Sako, Four-step commutation strategy of PWM rectifier of converter without DC-Link components for induction motor drive, in: Proceedings of the IEMDC, 2001, pp. 770–772.
[3] J.W. Kolar, F. Schafmeister, S.D. Round, H. Ertl, Novel three-phase AC–AC sparse matrix converters, IEEE Transactions on Power Electronics 22 (5) (2007) 1649–1661.
[4] L. Wei, T.A. Lipo, A novel matrix converter topology with simple commutation, in: Proceedings of the IEEE-IAS, vol. 3, 2001, pp. 1749–1754.
[5] L. Wei, T.A. Lipo, C. Ho, Matrix converter topologies with reduced number of switches, Proceedings of the PESC'03 vol. 3 (2002) 57–63.
[6] A. Jahangiri, A. Radan, M. Haghshenas, Synchronous control of indirect matrix converter for three-phase power conditioner, Electric Power Systems Research 80 (7) (2010) 857–868.
[7] S. Kwak, Indirect matrix converter drives for unity displacement factor and minimum switching losses, Electric Power Systems Research 77 (5) (2007) 447–454.
[8] H.K. Ardakani, A. Mousavinia, A. Jahangiri, A. Radan, Sawtooth switching strategy implementation for indirect matrix converter, in: Proceedings of the Power Electronics and Drive Systems Technology, PEDSTC, 2012, pp. 13–17.
[9] S. Li, F. Liu, Y. Zhong, X. Xing, J. Lu, Improving voltage transfer ratio of matrix converter employing single-mode and two-mode over modulation technology, in: Proceedings of the ICICTA'09, 2009, pp. 71–74.
[10] T. Wijekoon, C. Klumpner, et al., Implementation of a hybrid AC–AC direct power converter with unity voltage transfer, IEEE Transactions on Power Electronics 23 (2008) 1918–1926.
[11] P. Song, J. Lin, A hybrid AC–DC–AC matrix converter with a boost circuit, in: Proceedings of the ICEMI'09, vol. 2, 2009, pp. 416–421.
[12] Z. Li, X. Kong, X. Li, A novel over modulation strategy for two-stage matrix converter, in: Proceedings of the ICMTMA'09, 2009, pp. 617–620.
[13] T. Wijekoon, C. Klumpner, P. Wheeler, Improvement of output voltage capability of a two stage direct power converter under unbalanced input voltages, in: Proceedings of the EPE'05, 2005, p. 14.
[14] C. Klumpner, A hybrid indirect matrix converter immune to unbalanced voltage supply, with reduced switching losses and improved voltage transfer ratio, in: Proceedings of the APEC'06, 2006, pp. 133–139.
[15] W. Song, Y. Zhong, A study of z-source matrix converter with high voltage transfer ratio, in: Proceedings of the VPPC'08, 2008, pp. 1–6.
[16] K. Park, K.B. Lee, F. Blaabjerg, Improving output performance of a Z-source sparse matrix converter under unbalanced input-voltage conditions, IEEE Transactions on Power Electronics 27 (4) (2012) 2043–2054.
[17] X. Liu, P.C. Loh, P. Wang, F. Blaabjerg, Distributed generation using indirect matrix converter in boost operating mode, in: Proceedings of the Power Electronics and Drive Systems, PEDS, 2011, pp. 121–127.
[18] S.A.K. Bhat, J. Vithayathil, A simple multiple pulse width modulated ac chopper, IEEE Transactions on Industrial Electronics 29 (1982) 185–189.
[19] L. Huber, D. BorojeviC, Space vector modulated three-phase to three-phase matrix converter with input power factor correction, IEEE Transactions on Industry Applications 31 (1995) 1234–1246.
[20] A. Jahangiri, A. Radan, M. Haghshenas, Comparison of three switching strategies for indirect matrix converter, in: Proceedings of the EPE'09, 2009, pp. 1–9.
[21] IEC. IEC 61000-3-2: Electromagnetic compatibility (EMC) – Part 3: Limits – Section 2: Limits for Greater Than harmonic current emissions (equipment input current ≤ 16 A per phase), 2001, pp. 47.